Supporting information to

Late Pleistocene glaciation history of the southern Black Forest, Germany: ^{10}Be cosmic-ray exposure dating and equilibrium line altitude reconstructions in Sankt Wilhelmer Tal

Felix Martin Hofmann,

Frank Preusser,

Irene Schimmelpfennig,

Laëtitia Léanni,

ASTER Team (Georges Aumaître, Karim Keddadouche & Fawzi Zaidi)

Appendix S1: Detailed sample documentation

KS: Katzensteig; SW: Sankt Wilhelmer Tal

KS-1a

Coordinates (WGS 1984 coordinate system)		7.950002 °E 47.880995 °N
Elevation (m above sea-level)		1039
Context		Boulder on the proximal side of a terminal moraine of the ice-marginal position 1 in the Katzensteig cirque
Lithology		Migmatite
Dimensions: length, width and height (m)		3.50 x 3.50 x 3.80
Strike/dip of the sampled surface (°)		270/15
Height above ground of the sampled surface (m)		3.75
Sample thickness (cm)		1.8
Topographic shielding factor	Balco (2018)	0.969944
	Li (2018)	0.970214

Photo of the KS-1a boulder.

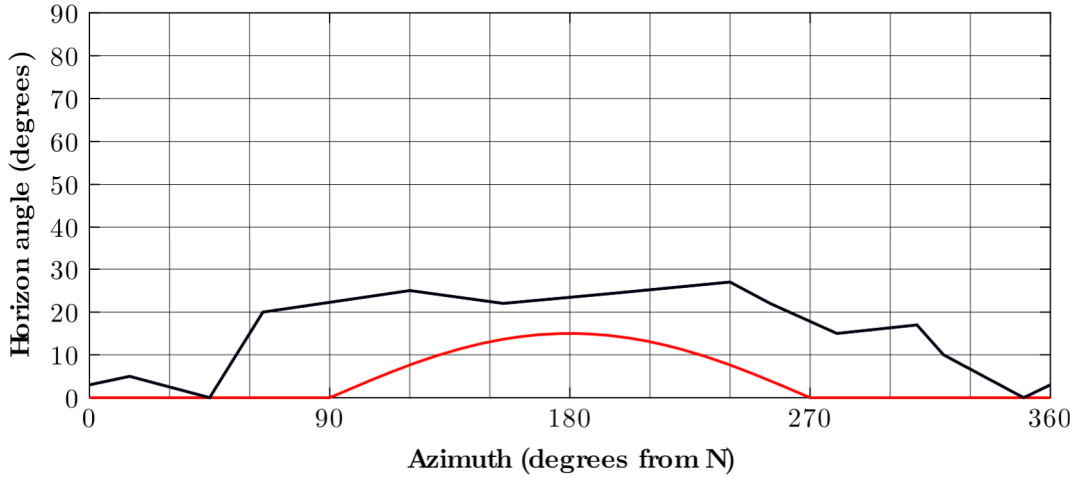

Horizon around the sampling surface on the KS-1a boulder. The blue line corresponds to the far-field horizon. The red line shows the near-field horizon implied by the dip of the sampling surface. The combined horizon is highlighted as black line.

KS-1b

Coordinates (WGS 1984 coordinate system)		7.947639 °E 47.882771 °N
Elevation (m above sea-level)		1019
Context		Boulder on a terminal moraine of the ice-marginal position 1 (?) in the Katzensteig cirque
Lithology		Migmatite
Dimensions: length, width and height (m)		2.80 x 2.70 x 2.50
Strike/dip of the sampled surface (°)		310/25
Height above ground of the sampled surface (m)		2.30
Sample thickness (cm)		2.6
Topographic shielding factor	Balco (2018)	0.961717
	Li (2018)	0.948215

Photo of the KS-1b boulder.

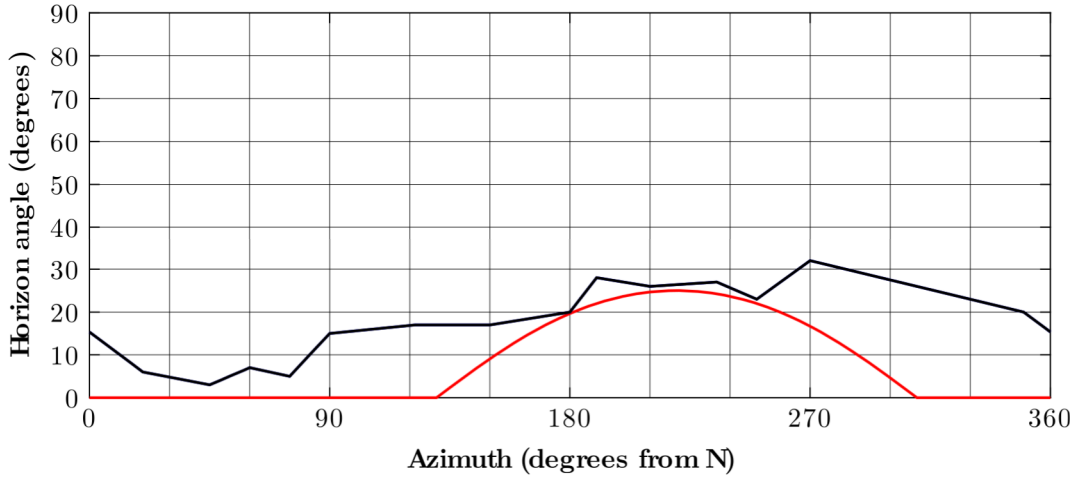

Horizon around the sampling surface on the KS-1b boulder. The blue line corresponds to the far-field horizon. The red line shows the near-field horizon implied by the dip of the sampling surface. The combined horizon is highlighted as black line.

KS-2a

Coordinates (WGS 1984 coordinate system)		7.948489 °E 47.883475 °N
Elevation (m above sea-level)		1017
Context		Boulder on the proximal side of a terminal moraine of the ice-marginal position 2 in the Katzensteig cirque
Lithology		Gneiss
Dimensions: length, width and height (m)		2.60 x 1.40 x 1.50
Strike/dip of the sampled surface (°)		265/5
Height above ground of the sampled surface (m)		1.45
Sample thickness (cm)		1.8
Topographic shielding factor	Balco (2018)	0.973091
	Li (2018)	0.960367

Photo of the KS-2a boulder.

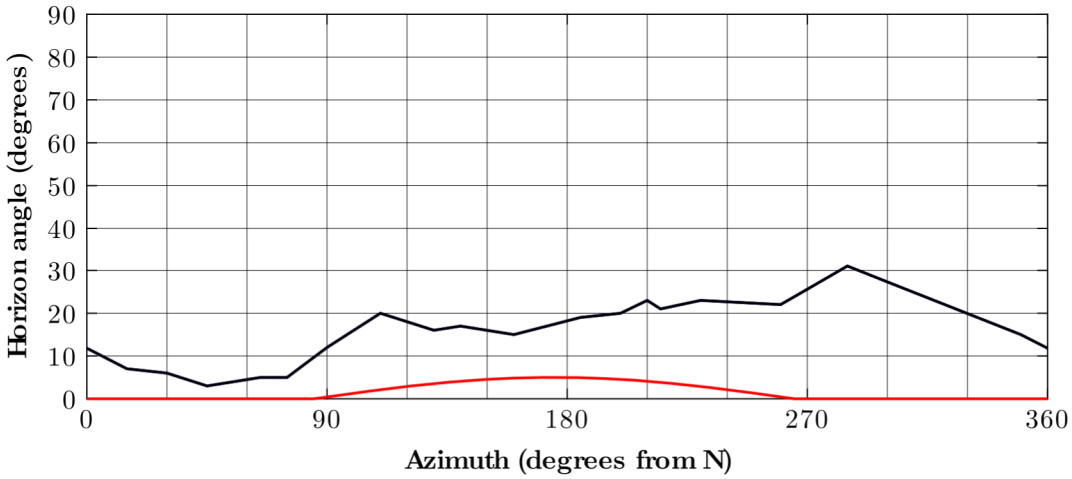

Horizon around the sampling surface on the KS-2a boulder. The blue line corresponds to the far-field horizon. The red line shows the near-field horizon implied by the dip of the sampling surface. The combined horizon is highlighted as black line.

KS-2b

Coordinates (WGS 1984 coordinate system)		7.949545 °E 47.883464 °N
Elevation (m above sea-level)		1010
Context		Boulder on the proximal side of a terminal moraine (frontal position) of the ice-marginal position 2 in the Katzensteig cirque
Lithology		Gneiss
Dimensions: length, width and height (m)		3.50 x 3.30 x 1.35
Strike/dip of the sampled surface (°)		320/5
Height above ground of the sampled surface (m)		1.30
Sample thickness (cm)		2.1
Topographic shielding factor	Balco (2018)	0.984485
	Li (2018)	0.982749

Photo of the KS-2b boulder.

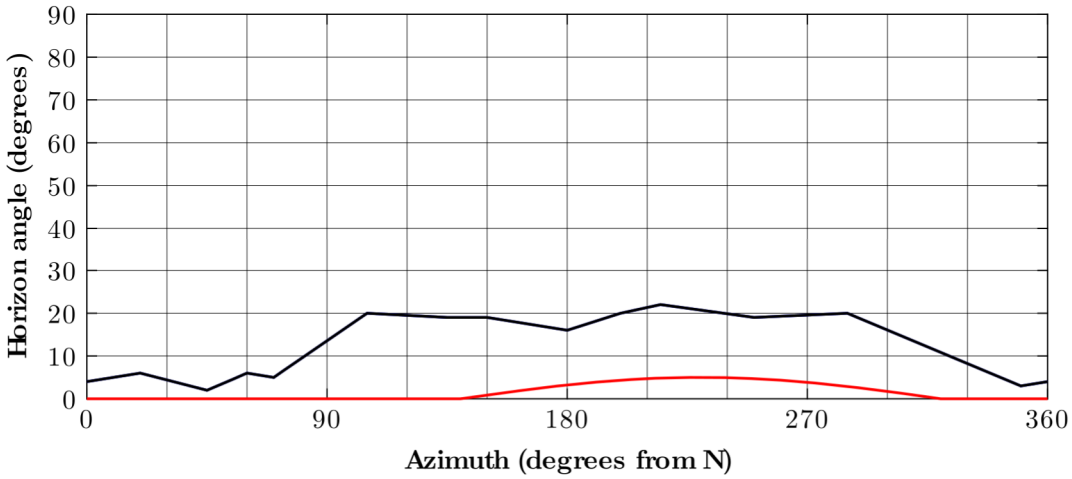

Horizon around the sampling surface on the KS-2b boulder. The blue line corresponds to the far-field horizon. The red line shows the near-field horizon implied by the dip of the sampling surface. The combined horizon is highlighted as black line.

KS-2c

Coordinates (WGS 1984 coordinate system)		7.950439 °E 47.883693 °N
Elevation (m above sea-level)		1011
Context		Boulder on the distal side of a terminal moraine (frontal position) of the ice-marginal position 2 in the Katzensteig cirque
Lithology		Gneiss
Dimensions: length, width and height (m)		3.60 x 2.15 x 1.30
Strike/dip of the sampled surface (°)		210/10
Height above ground of the sampled surface (m)		1.15
Sample thickness (cm)		2.2
Topographic shielding factor	Balco (2018)	0.986273
	Li (2018)	0.983238

Photo of the KS-2c boulder.

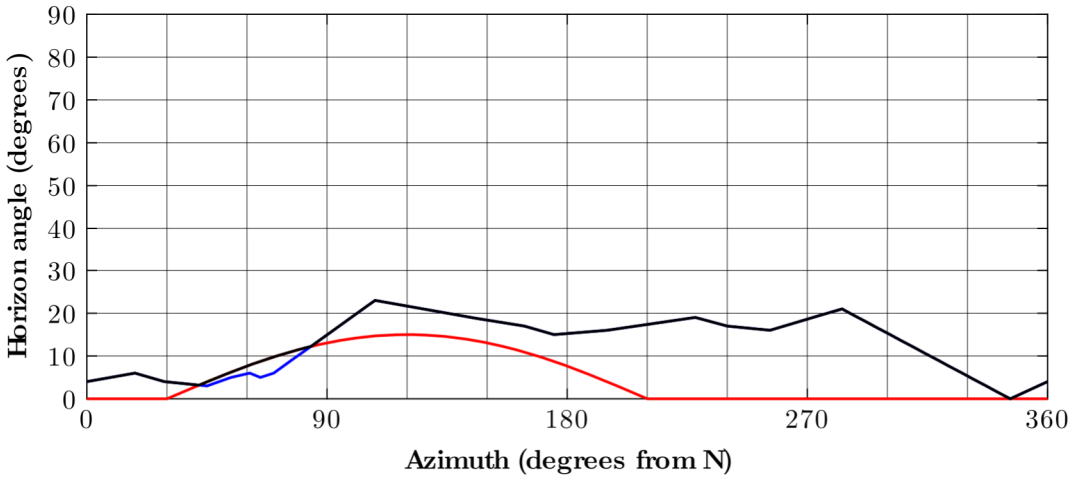

Horizon around the sampling surface on the KS-2c boulder. The blue line corresponds to the far-field horizon. The red line shows the near-field horizon implied by the dip of the sampling surface. The combined horizon is highlighted as black line.

KS-2d

Coordinates (WGS 1984 coordinate system)		7.950471 °E 47.883615 °N
Elevation (m above sea-level)		1013
Context		Boulder on the crest of a terminal moraine (frontal position)of the ice-marginal position 2 in the Katzensteig cirque
Lithology		Migmatite
Dimensions: length, width and height (m)		1.90 x 1.60 x 1.00
Strike/dip of the sampled surface (°)		200/10
Height above ground of the sampled surface (m)		0.95
Sample thickness (cm)		1.9
Topographic shielding factor	Balco (2018)	0.987129
	Li (2018)	0.983379

Photo of the KS-2d boulder.

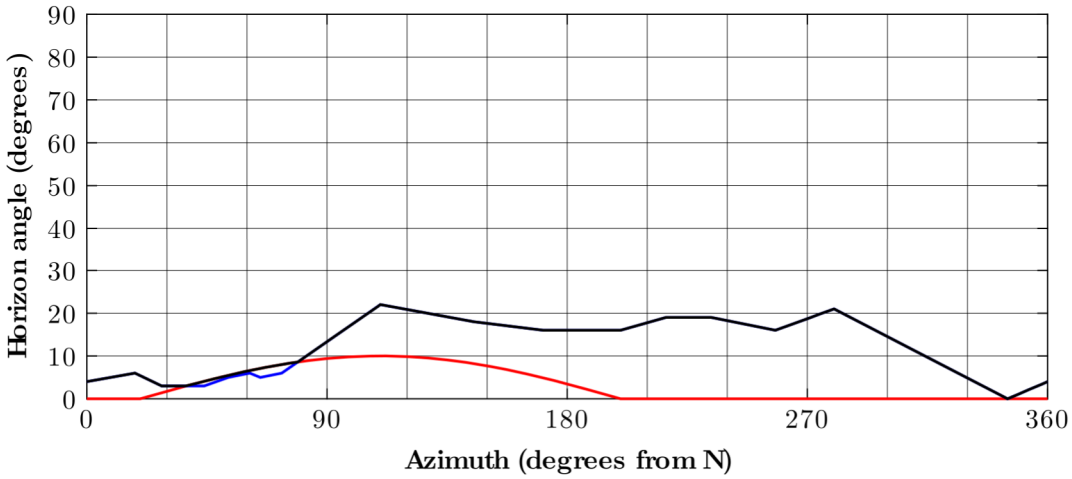

Horizon around the sampling surface on the KS-2d boulder. The blue line corresponds to the far-field horizon. The red line shows the near-field horizon implied by the dip of the sampling surface. The combined horizon is highlighted as black line.

KS-2e

Coordinates (WGS 1984 coordinate system)		7.950357 °E 47.883608 °N
Elevation (m above sea-level)		1013
Context		Boulder on the crest of a terminal moraine (frontal position) of the ice-marginal position 2 in the Katzensteig cirque
Lithology		Gneiss
Dimensions: length, width and height (m)		2.15 x 1.95 x 1.05
Strike/dip of the sampled surface (°)		90/20
Height above ground of the sampled surface (m)		1.05
Sample thickness (cm)		1.9
Topographic shielding factor	Balco (2018)	0.978584
	Li (2018)	0.977940

Photo of the KS-2e boulder.

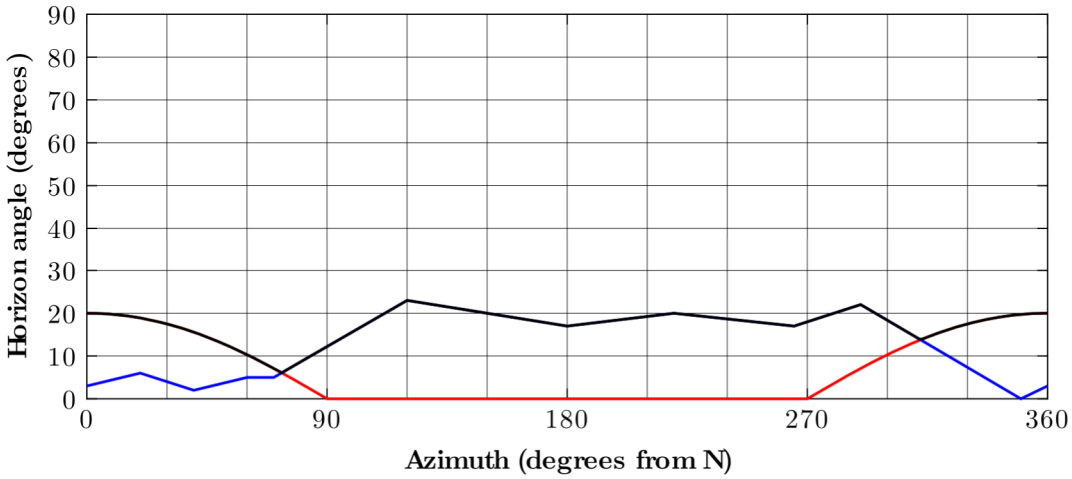

Horizon around the sampling surface on the KS-2e boulder. The blue line corresponds to the far-field horizon. The red line shows the near-field horizon implied by the dip of the sampling surface. The combined horizon is highlighted as black line.

KS-2f

Coordinates (WGS 1984 coordinate system)		7.948615 °E 47.883602 °N
Elevation (m above sea-level)		1018
Context		Boulder on the crest of a terminal moraine (lateral position) of the ice-marginal position 2 in the Katzensteig cirque
Lithology		Gneiss
Dimensions: length, width and height (m)		2.70 x 1.30 x 1.70
Strike/dip of the sampled surface (°)		180/10
Height above ground of the sampled surface (m)		1.65
Sample thickness (cm)		2.1
Topographic shielding factor	Balco (2018)	0.977411
	Li (2018)	0.973167

Photo of the KS-2f boulder.

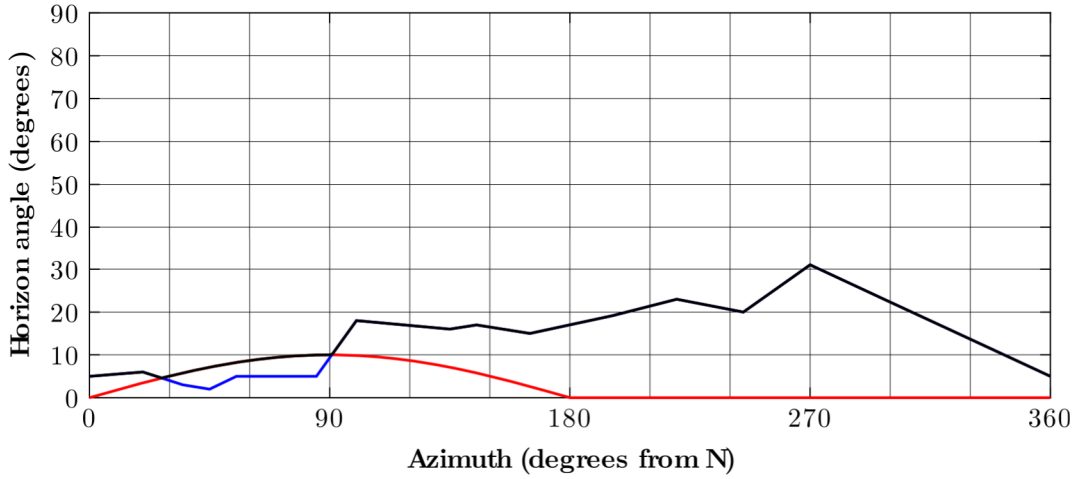

Horizon around the sampling surface on the KS-2f boulder. The blue line corresponds to the far-field horizon. The red line shows the near-field horizon implied by the dip of the sampling surface. The combined horizon is highlighted as black line.

KS-2g

Coordinates (WGS 1984 coordinate system)		7.949847 °E 47.883334 °N
Elevation (m above sea-level)		1010
Context		Boulder on the proximal side of a terminal moraine (frontal position) of the ice-marginal position 2 in the Katzensteig cirque
Lithology		Gneiss
Dimensions: length, width and height (m)		2.70 x 1.80 x 1.80
Strike/dip of the sampled surface (°)		300/5
Height above ground of the sampled surface (m)		1.75
Sample thickness (cm)		1.8
Topographic shielding factor	Balco (2018)	0.981684
	Li (2018)	0.982734

Photo of the KS-2g boulder.

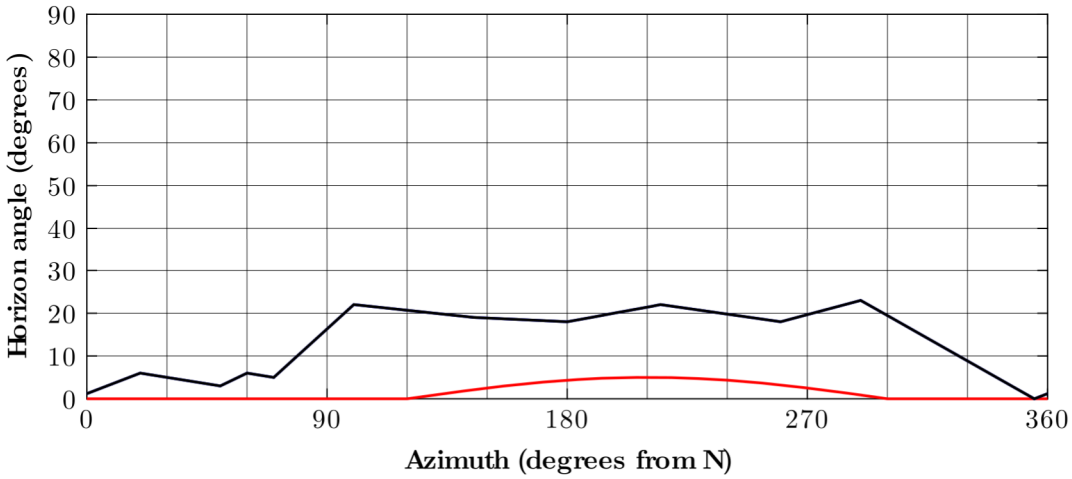

Horizon around the sampling surface on the KS-2g boulder. The blue line corresponds to the far-field horizon. The red line shows the near-field horizon implied by the dip of the sampling surface. The combined horizon is highlighted as black line.

KS-3a

Coordinates (WGS 1984 coordinate system)		7.950995 °E 47.883767 °N
Elevation (m above sea-level)		1006
Context		Boulder on the distal side of a terminal moraine (frontal position) of the ice-marginal position 3 in the Katzensteig cirque
Lithology		Gneiss
Dimensions: length, width and height (m)		2.05 x 1.55 x 1.30
Strike/dip of the sampled surface (°)		290/5
Height above ground of the sampled surface (m)		1.30
Sample thickness (cm)		1.9
Topographic shielding factor	Balco (2018)	0.984652
	Li (2018)	0.980652

Photo of the KS-3a boulder.

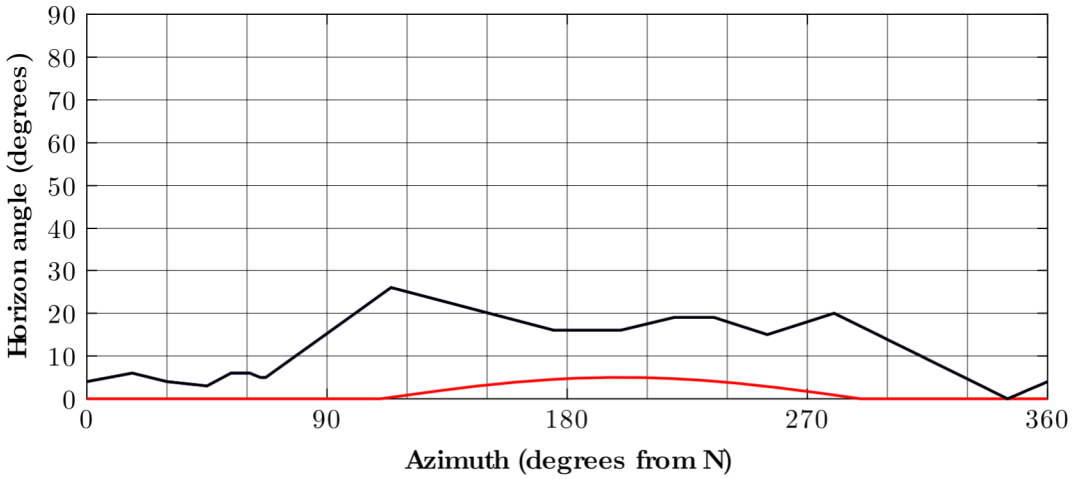

Horizon around the sampling surface on the KS-3a boulder. The blue line corresponds to the far-field horizon. The red line shows the near-field horizon implied by the dip of the sampling surface. The combined horizon is highlighted as black line.

SW-2

Coordinates (WGS 1984 coordinate system)		7.983656 °E 47.882025 °N
Elevation (m above sea-level)		910
Context		Boulder on the proximal side of a terminal moraine (frontal position) of the ice-marginal position 2 in Sankt Wilhelmer Tal
Lithology		Migmatite
Dimensions: length, width and height (m)		2.90 x 2.70 x 2.20
Strike/dip of the sampled surface (°)		0/0
Height above ground of the sampled surface (m)		2.20
Sample thickness (cm)		2.8
Topographic shielding factor	Balco (2018)	0.947675
	Li (2018)	0.956313

Photo of the SW-2 boulder.

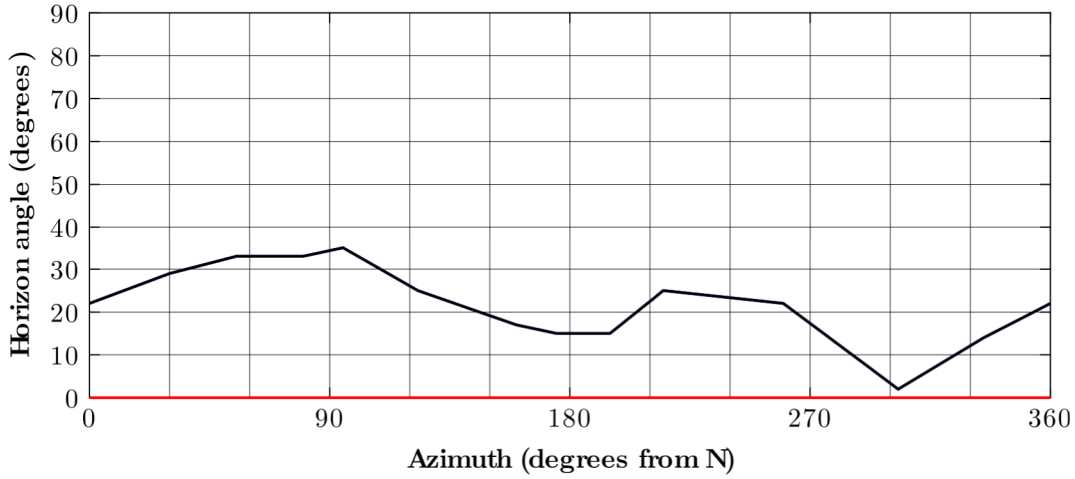

Horizon around the sampling surface on the SW-2 boulder. The blue line corresponds to the far-field horizon. The red line shows the near-field horizon implied by the dip of the sampling surface. The combined horizon is highlighted as black line.

SW-9

Coordinates (WGS 1984 coordinate system)		7.959058 °E 47.891912 °N
Elevation (m above sea-level)		789
Context		Boulder on the crest of a terminal moraine (lateral position) of the ice-marginal position 9 in Sankt Wilhelmer Tal
Lithology		Migmatite
Dimensions: length, width and height (m)		2.10 x 1.40 x 1.20
Strike/dip of the sampled surface (°)		250/35
Height above ground of the sampled surface (m)		1.00
Sample thickness (cm)		2.7
Topographic shielding factor	Balco (2018)	0.944719
	Li (2018)	0.941004

Photos of the SW-9 boulder.

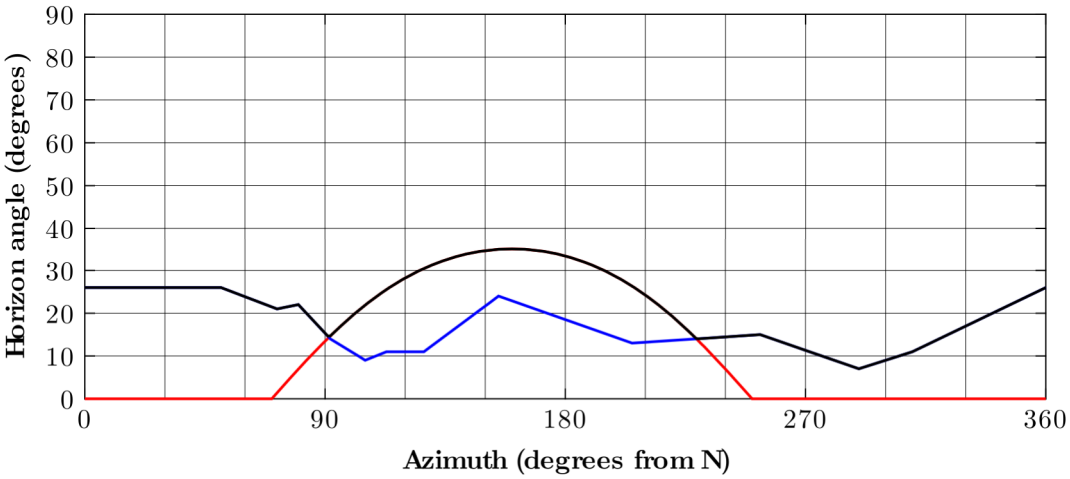

Horizon around the sampling surface on the SW-9 boulder. The blue line corresponds to the far-field horizon. The red line shows the near-field horizon implied by the dip of the sampling surface. The combined horizon is highlighted as black line.

SW-10

Coordinates (WGS 1984 coordinate system)		7.957121 °E 47.891928 °N
Elevation (m above sea-level)		777
Context		Boulder on the crest of a terminal moraine (latero-frontal position) of the ice-marginal position 10 in Sankt Wilhelmer Tal
Lithology		Migmatite
Dimensions: length, width and height (m)		3.70 x 2.10 x 1.10
Strike/dip of the sampled surface (°)		80/15
Height above ground of the sampled surface (m)		1.05
Sample thickness (cm)		2.8
Topographic shielding factor	Balco (2018)	0.974701
	Li (2018)	0.953857

Photo of the SW-10 boulder.

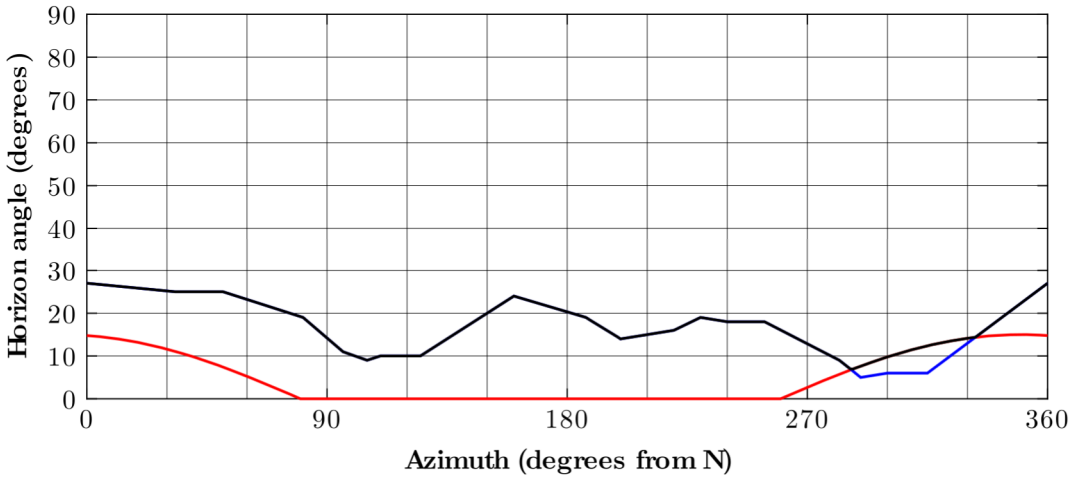

Horizon around the sampling surface on the SW-10 boulder. The blue line corresponds to the far-field horizon. The red line shows the near-field horizon implied by the dip of the sampling surface. The combined horizon is highlighted as black line.

SW-11a

Coordinates (WGS 1984 coordinate system)		7.954207 °E 47.892901 °N
Elevation (m above sea-level)		759
Context		Boulder on the crest of a terminal moraine (latero-frontal position) of the ice-marginal position 11 in Sankt Wilhelmer Tal
Lithology		Migmatite
Dimensions: length, width and height (m)		3.70 x 1.90 x 1.00
Strike/dip of the sampled surface (°)		340/15
Height above ground of the sampled surface (m)		0.95
Sample thickness (cm)		2.5
Topographic shielding factor	Balco (2018)	0.974568
	Li (2018)	0.967416

Photo of the SW-11a boulder.

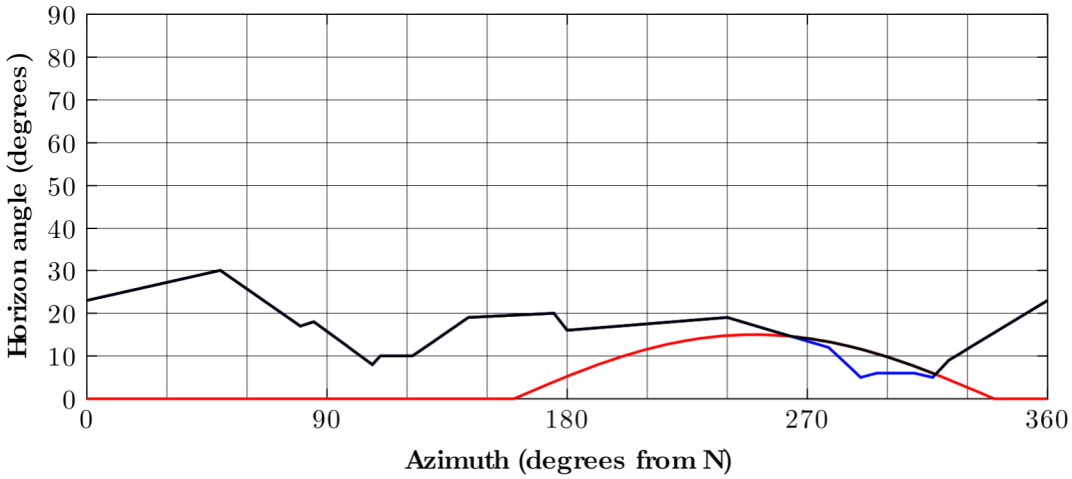

Horizon around the sampling surface on the SW-11a boulder. The blue line corresponds to the far-field horizon. The red line shows the near-field horizon implied by the dip of the sampling surface. The combined horizon is highlighted as black line.

SW-11b

Coordinates (WGS 1984 coordinate system)		7.953907 °E 47.893093 °N
Elevation (m above sea-level)		758
Context		Boulder on the distal side of a terminal moraine (latero-frontal position) of the ice-marginal position 11 in Sankt Wilhelmer Tal
Lithology		Migmatite
Dimensions: length, width and height (m)		1.90 x 1.20 x 1.40
Strike/dip of the sampled surface (°)		200/5
Height above ground of the sampled surface (m)		1.40
Sample thickness (cm)		2.7
Topographic shielding factor	Balco (2018)	0.971608
	Li (2018)	0.967011

Photo of the SW-11b boulder.

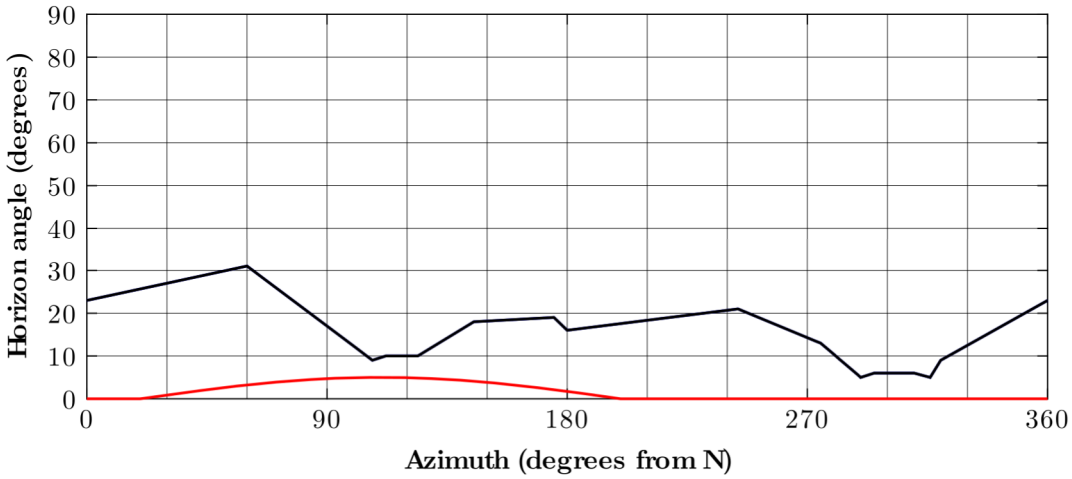

Horizon around the sampling surface on the SW-11b boulder. The blue line corresponds to the far-field horizon. The red line shows the near-field horizon implied by the dip of the sampling surface. The combined horizon is highlighted as black line.

SW-11c

Coordinates (WGS 1984 coordinate system)		7.953808 °E 47.893038 °N
Elevation (m above sea-level)		757
Context		Boulder on the distal side of a terminal moraine (latero-frontal position) of the ice-marginal position 11 in Sankt Wilhelmer Tal
Lithology		Migmatite
Dimensions: length, width and height (m)		2.70 x 2.00 x 1.70
Strike/dip of the sampled surface (°)		60/15
Height above ground of the sampled surface (m)		1.65
Sample thickness (cm)		2.8
Topographic shielding factor	Balco (2018)	0.975586
	Li (2018)	0.967081

Photo of the SW-11c boulder.

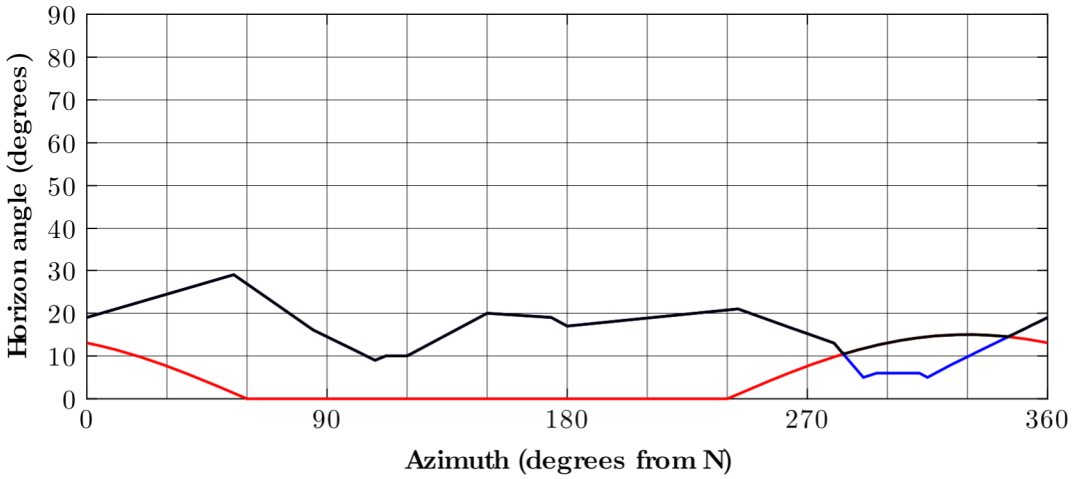

Horizon around the sampling surface on the SW-11c boulder. The blue line corresponds to the far-field horizon. The red line shows the near-field horizon implied by the dip of the sampling surface. The combined horizon is highlighted as black line.

SW-11d

Coordinates (WGS 1984 coordinate system)		7.953791 °E 47.893185 °N
Elevation (m above sea-level)		755
Context		Boulder on the distal side of a terminal moraine (latero-frontal position) of the ice-marginal position 11 in Sankt Wilhelmer Tal
Lithology		Migmatite
Dimensions: length, width and height (m)		1.80 x 1.50 x 1.30
Strike/dip of the sampled surface (°)		90/40
Height above ground of the sampled surface (m)		1.20
Sample thickness (cm)		2.5
Topographic shielding factor	Balco (2018)	0.931333
	Li (2018)	0.927845

Photo of the SW-11d boulder.

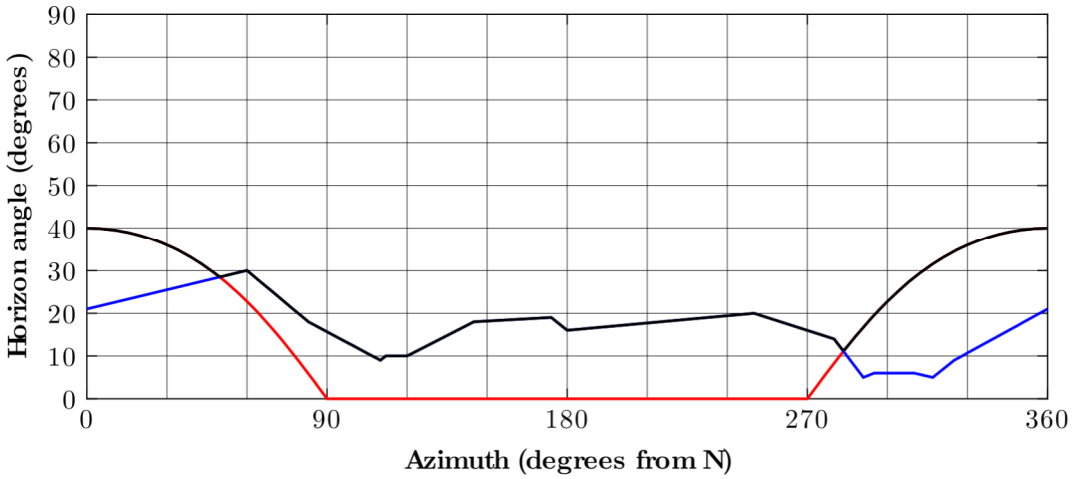

Horizon around the sampling surface on the SW-11d boulder. The blue line corresponds to the far-field horizon. The red line shows the near-field horizon implied by the dip of the sampling surface. The combined horizon is highlighted as black line.

SW-12a

Coordinates (WGS 1984 coordinate system)		7.953460 °E 47.892540 °N
Elevation (m above sea-level)		766
Context		Boulder on the crest of a terminal moraine (latero-frontal position) of the ice-marginal position 12 in Sankt Wilhelmer Tal
Lithology		Migmatite
Dimensions: length, width and height (m)		3.60 x 2.60 x 1.70
Strike/dip of the sampled surface (°)		40/20
Height above ground of the sampled surface (m)		1.65
Sample thickness (cm)		2.4
Topographic shielding factor	Balco (2018)	0.976411
	Li (2018)	0.967224

Photo of the SW-12a boulder.

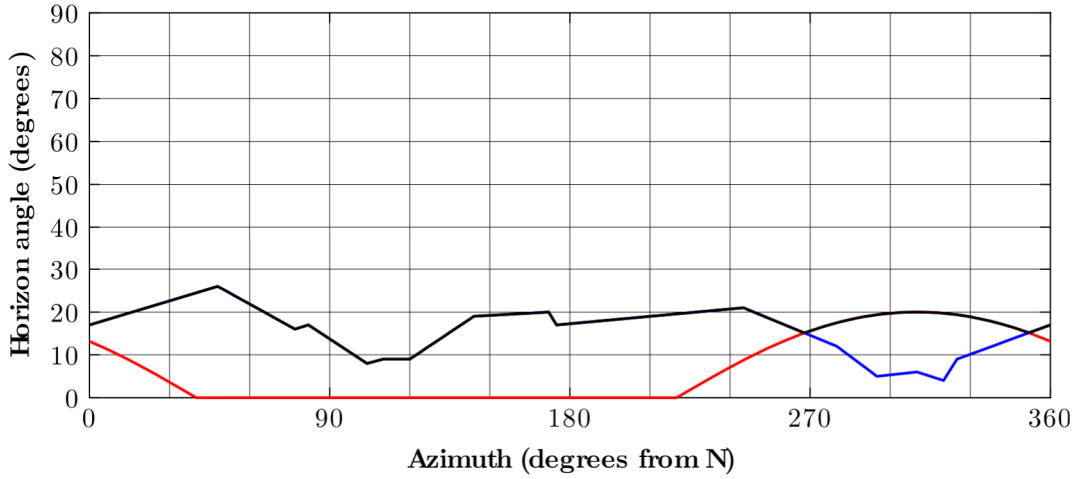

Horizon around the sampling surface on the SW-12a boulder. The blue line corresponds to the far-field horizon. The red line shows the near-field horizon implied by the dip of the sampling surface. The combined horizon is highlighted as black line.

SW-15a

Coordinates (WGS 1984 coordinate system)		7.946590 °E 47.891977 °N
Elevation (m above sea-level)		919
Context		Boulder on the crest of a terminal moraine (lateral position) of the ice-marginal position 15 in Sankt Wilhelmer Tal
Lithology		Migmatite
Dimensions: length, width and height (m)		3.10 x 1.90 x 1.50
Strike/dip of the sampled surface (°)		100/20
Height above ground of the sampled surface (m)		1.45
Sample thickness (cm)		2.1
Topographic shielding factor	Balco (2018)	0.981034
	Li (2018)	0.970717

Photo of the SW-15a boulder.

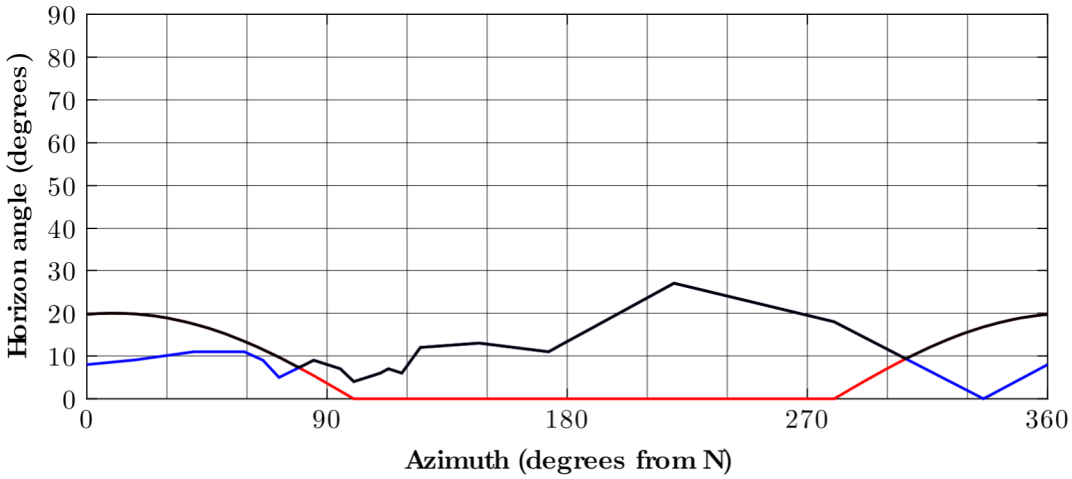

Horizon around the sampling surface on the SW-15a boulder. The blue line corresponds to the far-field horizon. The red line shows the near-field horizon implied by the dip of the sampling surface. The combined horizon is highlighted as black line.

SW-15b

Coordinates (WGS 1984 coordinate system)		7.946578 °E 47.891899 °N
Elevation (m above sea-level)		919
Context		Boulder on the crest of a terminal moraine (lateral position) of the ice-marginal position 15 in Sankt Wilhelmer Tal
Lithology		Migmatite
Dimensions: length, width and height (m)		4.20 x 1.90 x 2.20
Strike/dip of the sampled surface (°)		110/25
Height above ground of the sampled surface (m)		2.10
Sample thickness (cm)		2.1
Topographic shielding factor	Balco (2018)	0.976074
	Li (2018)	0.963193

Photo of the SW-15b boulder.

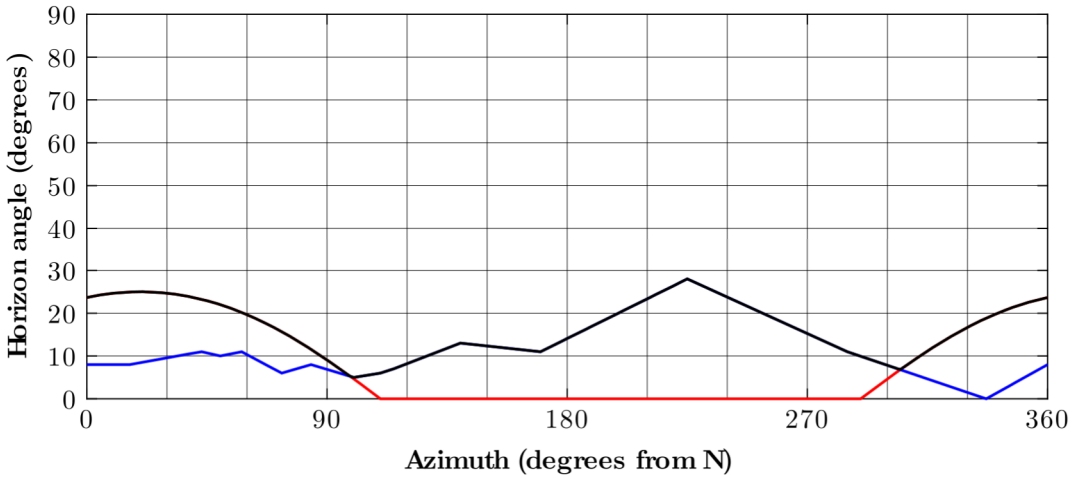

Horizon around the sampling surface on the SW-15b boulder. The blue line corresponds to the far-field horizon. The red line shows the near-field horizon implied by the dip of the sampling surface. The combined horizon is highlighted as black line.

SW-16

Coordinates (WGS 1984 coordinate system)		7.944610 °E 47.893502 °N
Elevation (m above sea-level)		916
Context		Boulder on the proximal side of a terminal moraine (lateral position) of the ice-marginal position 16 in Sankt Wilhelmer Tal
Lithology		Migmatite
Dimensions: length, width and height (m)		2.10 x 1.00 x 1.00
Strike/dip of the sampled surface (°)		290/25
Height above ground of the sampled surface (m)		0.90
Sample thickness (cm)		2.1
Topographic shielding factor	Balco (2018)	0.982982
	Li (2018)	0.984388

Photo of the SW-16 boulder.

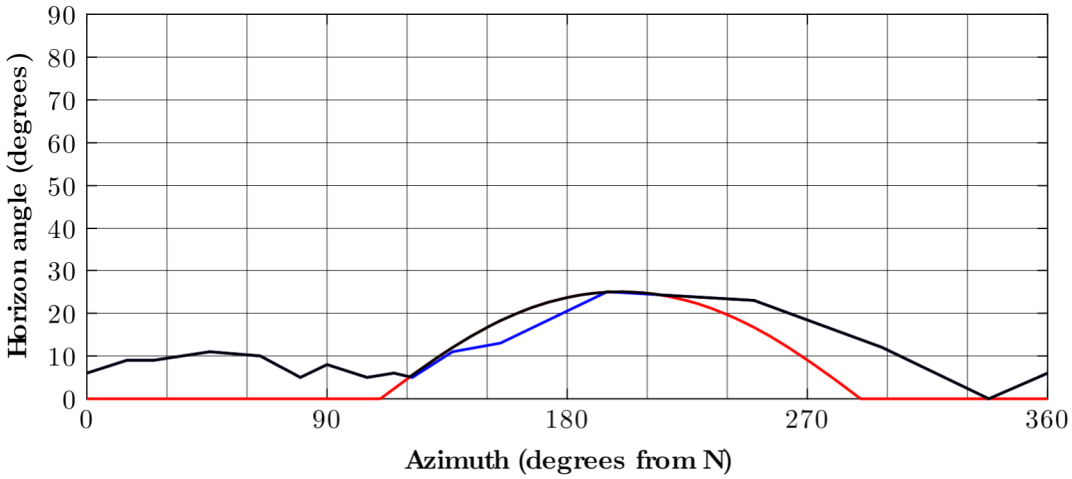

Horizon around the sampling surface on the SW-16 boulder. The blue line corresponds to the far-field horizon. The red line shows the near-field horizon implied by the dip of the sampling surface. The combined horizon is highlighted as black line.

SW-17

Coordinates (WGS 1984 coordinate system)		7.943865 °E 47.892935 °N
Elevation (m above sea-level)		934
Context		Boulder on the proximal side of a terminal moraine (lateral position) of the ice-marginal position 17 in Sankt Wilhelmer Tal
Lithology		Migmatite
Dimensions: length, width and height (m)		4.30 x 3.10 x 2.00
Strike/dip of the sampled surface (°)		270/35
Height above ground of the sampled surface (m)		1.95
Sample thickness (cm)		2.2
Topographic shielding factor	Balco (2018)	Not determined, as the boulder is located in a dense coniferous forest
	Li (2018)	0.958618

Photo of the SW-17 boulder.

SW-18a

Coordinates (WGS 1984 coordinate system)		7.932353 °E 47.901610 °N
Elevation (m above sea-level)		655
Context		Boulder on a medial moraine of the ice-marginal position 18 in Sankt Wilhelmer Tal
Lithology		Migmatite
Dimensions: length, width and height (m)		4.00 x 2.00 x 1.70
Strike/dip of the sampled surface (°)		160/40
Height above ground of the sampled surface (m)		1.70
Sample thickness (cm)		1.9
Topographic shielding factor	Balco (2018)	0.893304
	Li (2018)	0.898342

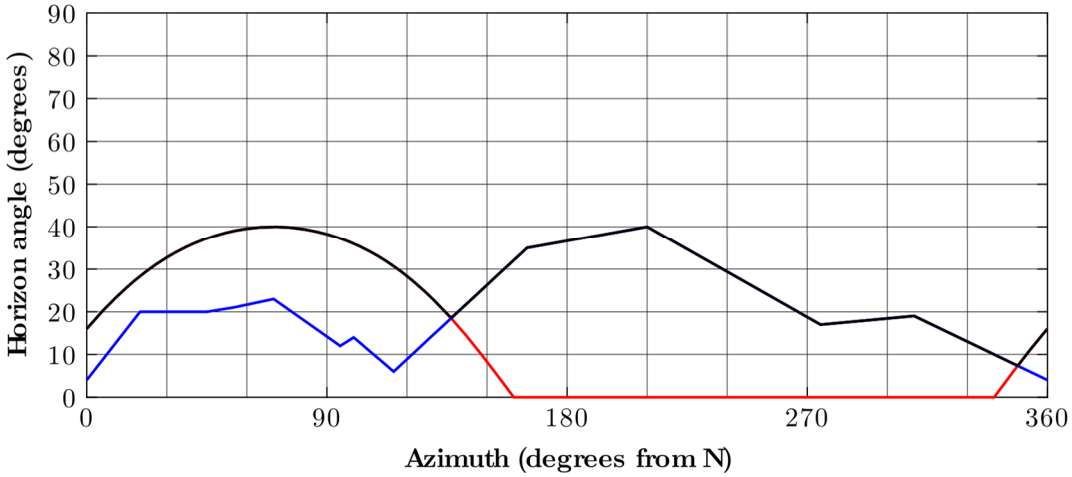

Horizon around the sampling surface on the SW-18a boulder. The blue line corresponds to the far-field horizon. The red line shows the near-field horizon implied by the dip of the sampling surface. The combined horizon is highlighted as black line.

SW-18b

Coordinates (WGS 1984 coordinate system)		7.932376 °E 47.901672 °N
Elevation (m above sea-level)		653
Context		Boulder on a medial moraine of the ice-marginal position 18 in Sankt Wilhelmer Tal
Lithology		Migmatite
Dimensions: length, width and height (m)		2.70 x 1.40 x 1.80
Strike/dip of the sampled surface (°)		90/25
Height above ground of the sampled surface (m)		1.80
Sample thickness (cm)		1.6
Topographic shielding factor	Balco, 2018	Balco (2018)
	Li, 2018	Li (2018)

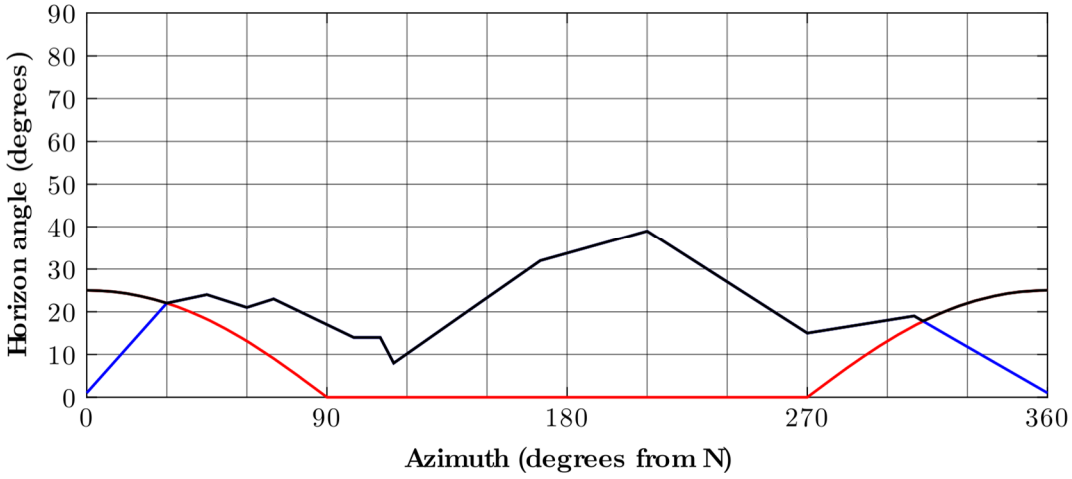

Horizon around the sampling surface on the SW-18b boulder. The blue line corresponds to the far-field horizon. The red line shows the near-field horizon implied by the dip of the sampling surface. The combined horizon is highlighted as black line.

SW-18c

Coordinates (WGS 1984 coordinate system)		7.931987 °E 47.901887 °N
Elevation (m above sea-level)		654
Context		Boulder on a medial moraine of the ice-marginal position 18 in Sankt Wilhelmer Tal
Lithology		Migmatite
Dimensions: length, width and height (m)		3.20 x 2.00 x 2.05
Strike/dip of the sampled surface (°)		100/45
Height above ground of the sampled surface (m)		2.00
Sample thickness (cm)		1.5
Topographic shielding factor	Balco (2018)	0.876899
	Li (2018)	0.880220

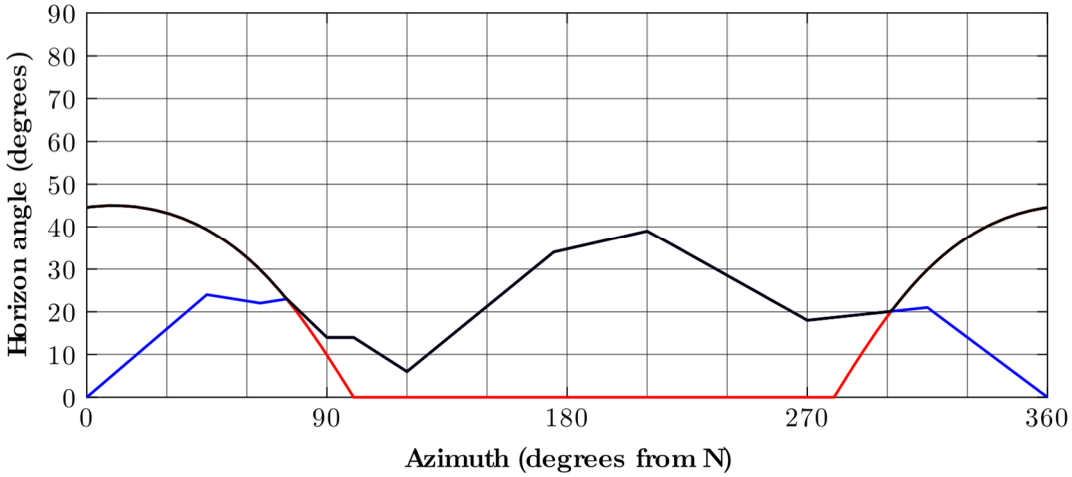

Horizon around the sampling surface on the SW-18c boulder. The blue line corresponds to the far-field horizon. The red line shows the near-field horizon implied by the dip of the sampling surface. The combined horizon is highlighted as black line.

Review of ^{10}Be cosmic-ray exposure (CRE) ages at key sites in the mountain regions of Central Europe and their forelands

If topographic shielding factors were not reported in the original publications, they were determined with a digital terrain model (DTM) acquired during the shuttle radar topography mission (SRTM) with a xy-resolution of about 30 m at the equator (NASA Jet Propulsion Laboratory, 2013) and the ESRI ArcGIS toolbox of Li (2018).

The ^{10}Be CRE ages were calculated on the 12th of July 2021 with the online CREp (cosmic-ray exposure program) calculator. This online calculator requires ^{10}Be concentrations computed with the 07KNSTD standardisation as input (Martin *et al.*, 2017). As most of the previously published ^{10}Be concentrations were calibrated against other standards, they were first recalculated with appropriate conversion factors. They were retrieved from a MATLAB script of version 2.3 of the online exposure age calculator, formerly known as the CRONUS-Earth online exposure age calculator (make_al_be_consts_v23.m; Balco, 2007).

The following parameters were chosen in the calculator:

- the time-dependent Lal/Stone scaling scheme (Nishiizumi *et al.*, 1989; Lal, 1991; Stone, 2000; Balco *et al.*, 2008),
- the ERA-40 atmosphere model (Uppala *et al.*, 2005), as suggested by Martin *et al.* (2017),
- the atmospheric ^{10}Be-based virtual dipole moment (Muscheler *et al.*, 2005)
- and the production rate calibrated by Claude *et al.* (2014).

The rock density was set to 2.65 g cm^{-3}. The CRE ages were not corrected for denudation and snow shielding. CRE ages were excluded as done by the authors. Landform ages were computed if two or more CRE ages were available from a landform. Reduced chi-squared (χ^2_R) statistic was performed for sets of at least three CRE ages. The critical value was retrieved from a standard chi-squared table ($P = 0.05$ and $df = n - 1$) and divided by the degrees of freedom. If χ^2_R is lower than the critical value, the hypothesis that the data form a single population cannot be excluded at 95% confidence (Spencer *et al.*, 2017). In this case the mean CRE age was chosen as landform age. If χ^2_R turns out to be higher than the critical value, analytical uncertainties do not fully account for the scatter in the CRE ages (Spencer *et al.*, 2017). In this case, the CRE age with the worst reduced chi-squared was discarded. This process was repeated until χ^2_R was lower than the critical value. The outliers are shown

in grey. Landform uncertainties were calculated as follows: the mean analytical uncertainty and the ^{10}Be production rate uncertainty were added in quadrature.

If two CRE ages were available from a landform, the mean CRE age was chosen as landform age. Landform age uncertainties were determined as for sets of at least three CRE ages. If only one CRE age was available from a landform, it was chosen as the landform age.

Table S1. Input-sheet for the online CREp calculator.

Boulder	Latitude (° N WGS 1984)	Longitude (° E WGS 1984)	Elevation (m above sea-level)	^{10}Be concentration (atoms g^{-1} quartz)	1σ ^{10}Be concentration uncertainty (atoms g^{-1} quartz)	Topographic shielding factor	Density (g cm^{-3})	Sample thickness (cm)	Denudation rate (cm a^{-1})
W7	48.00760	7.03830	525	88808	10050	0.97927	2.65	3.0	0
W8	48.01020	7.03770	550	84379	10130	0.96535	2.65	3.0	0
A6a	48.06110	7.05370	850	178500	12861	0.99500	2.65	3.0	0
A6b	48.06110	7.05370	850	184659	16776	0.92697	2.65	3.0	0
M5a	48.07470	7.04030	1100	166840	11896	0.80354	2.65	3.0	0
M5c	48.07470	7.04030	1100	166868	13708	0.87717	2.65	3.0	0
M5b	48.07470	7.04030	1100	155261	12953	0.85272	2.65	3.0	0
M5e	48.07560	7.04110	1100	154677	14388	0.94522	2.65	3.0	0
Ln2	48.11110	7.10040	990	136992	13867	0.99571	2.65	3.0	0
ER-1	47.16055	7.68767	580	150546	9124	1.00000	2.65	6.0	0
ER-2	47.15996	7.68391	585	141422	6204	0.92100	2.65	5.0	0
ER-8	47.14777	7.68379	595	147809	9124	1.00000	2.65	3.0	0
GS1	46.86640	7.47160	873	169900	13900	1.00000	2.65	2.0	0

GS3	46.85150	7.47440	937	168900	7700	1.00000	2.65	4.0	0
GS5	46.84940	7.47640	925	152700	3800	1.00000	2.65	4.0	0
BS2	46.88590	7.48860	729	138500	10300	1.00000	2.65	2.0	0
BS3	46.94240	7.50590	678	112500	5200	1.00000	2.65	4.0	0
BS4	46.93970	7.51560	732	110100	3400	1.00000	2.65	4.0	0
BS5	46.93930	7.52640	745	132000	3700	1.00000	2.65	4.0	0
BS6	46.94000	7.53050	762	136200	3500	1.00000	2.65	4.0	0
Reuss-21	47.39520	8.19465	446	124400	4900	1.00000	2.65	5.0	0
Reuss-20	47.34763	8.31435	502	111000	5400	1.00000	2.65	4.0	0
AVS-03-01	47.97465	11.42111	670	136769	7117	0.99700	2.65	5.6	0
AVS-03-06	47.98626	11.40085	650	125090	7025	1.00000	2.65	5.0	0
AVS-03-11	48.02109	11.39898	655	114232	6387	0.98700	2.65	5.0	0
AVS-03-22	47.98646	11.40338	685	118794	6752	0.99400	2.65	5.5	0
AVS-03-03	47.99515	11.38970	656	134488	6022	0.99700	2.65	5.5	0
AVS-03-04	47.95000	11.39167	659	118156	9306	0.99600	2.65	4.5	0
Gamma 3	47.07861	11.41722	1215	170619	8872	0.87800	2.65	4.0	0
Gamma 5	47.07861	11.41722	1220	171531	12350	0.87700	2.65	4.0	0

Gamma 8a	47.07861	11.41722	1215	110400	4195	0.50900	2.65	2.0	0
Gamma 103	47.07861	11.41722	1330	185217	6853	0.89100	2.65	4.0	0
BW-03-15	49.13000	13.12000	862	190692	6293	0.99700	2.65	3.5	0
BW-03-14	49.13000	13.12000	848	166969	11354	0.99700	2.65	4.0	0
BW-03-16	49.13000	13.12000	874	177918	6049	0.99700	2.65	4.0	0
BW-03-06	49.13265	13.12180	873	173356	7454	0.99700	2.65	4.5	0
BW-03-02	49.13192	13.12033	864	171531	7033	0.99600	2.65	4.5	0
BW-03-03	49.13205	13.11992	870	160582	6423	0.99600	2.65	4.0	0
BW-03-20	49.13000	13.12000	870	158758	5874	0.99500	2.65	4.5	0
BW-04-03	49.12869	13.11933	905	151458	6816	0.99600	2.65	3.5	0
BW-04-04	49.12803	13.12117	915	153283	15175	0.99600	2.65	3.5	0
BW-03-09	49.13000	13.12000	945	146896	6023	0.99700	2.65	4.0	0
LA-2	49.11310	13.33130	1090	163182	19111	0.99997	2.65	3.0	0
LA-1	49.11310	13.33030	1086	141682	12665	0.99997	2.65	3.0	0
PR-6	49.07840	13.40140	1048	166258	10873	0.99954	2.65	3.0	0
PR-7	49.07910	13.40200	1042	189600	21918	0.99970	2.65	3.0	0
PR-8	49.07940	13.40210	1038	165560	7848	0.99987	2.65	3.0	0

PR-2	49.07650	13.40190	1079	157084	6918	0.99984	2.65	3.0	0
PR-3	49.07680	13.40110	1079	161166	5947	0.99970	2.65	3.0	0
PR-1	49.07520	13.40210	1085	154457	5721	0.99984	2.65	3.0	0
PR-4	49.07660	13.40050	1085	142413	8975	0.99927	2.65	3.0	0
PR-5	49.07660	13.40040	1083	131878	15388	0.99927	2.65	3.0	0
SK-16	50.79213	15.55783	1055	189970	9354	0.99921	2.65	2.0	0
SK-03	50.79287	15.56898	1000	177097	8405	0.99969	2.65	3.0	0
SK-08	50.78660	15.56328	1208	219197	7064	0.99932	2.65	1.0	0
SK-09	50.78682	15.56304	1207	216294	6294	0.99948	2.65	1.0	0
SK-05	50.78362	15.56296	1240	132817	21003	0.99698	2.65	3.0	0
SK-07	50.78368	15.56274	1245	191279	6658	0.99887	2.65	3.0	0
SK-06	50.78170	15.56281	1253	143556	4861	0.99552	2.65	3.0	0
SK-01	50.78002	15.56250	1283	137094	9209	0.98584	2.65	3.0	0
SK-02	50.78033	15.56188	1273	140016	5851	0.98700	2.65	3.0	0
LN-19	50.74827	15.59388	830	149874	13109	0.98973	2.65	3.0	0
LN-20	50.74835	15.59413	828	143520	12277	0.98992	2.65	3.0	0
Lo-7	50.76174	15.72228	910	153259	8935	0.99900	2.65	3.0	0

Lo-6	50.76184	15.72106	924	153936	6038	0.99900	2.65	3.0	0
Lo-5	50.76237	15.71686	983	168119	6278	0.99900	2.65	3.0	0
Lo-3	50.75401	15.70461	1173	197129	5168	0.99900	2.65	3.0	0
Lo-4	50.75542	15.70336	1140	168956	5981	0.99900	2.65	3.0	0
Lo-2	50.75049	15.70129	1185	155164	10006	0.99600	2.65	3.0	0
G-18	50.71100	15.72000	987	144672	4448	0.99748	2.65	4.0	0
G-19	50.71000	15.72100	974	165054	5480	0.99905	2.65	3.0	0
G-20	50.70700	15.72700	914	123199	9521	0.99915	2.65	3.0	0
G-21	50.70700	15.72700	906	138368	4779	0.99917	2.65	3.0	0
G-10	50.71300	15.72100	947	126852	8314	0.99894	2.65	3.0	0
G-11	50.71300	15.72100	951	151575	17018	0.99870	2.65	3.0	0
G-12	50.71300	15.72100	961	123628	8073	0.99780	2.65	3.0	0
G-17	50.71800	15.72400	927	161780	5428	0.99487	2.65	3.0	0
G-24	50.71700	15.72500	925	129504	4203	0.99246	2.65	3.0	0
G-15	50.71900	15.72400	940	123407	4498	0.99348	2.65	4.0	0
G-16	50.71800	15.72400	932	153404	5505	0.99416	2.65	3.0	0
G-13	50.72200	15.72500	971	130270	4251	0.99582	2.65	2.0	0

G-14	50.72200	15.72500	966	135878	4211	0.99582	2.65	4.0	0
Lk-1	50.74740	15.74060	1053	153276	6183	0.99600	2.65	3.0	0

Table S2. Recalculated ^{10}Be CRE ages from terminal moraines at key sites in mountainous regions in Central Europe and their forelands. Outlying CRE ages identified via reduced chi-squared statistic are shown in grey.

Locality	Landform	Landform age (ka)	Oldest ^{10}Be CRE age (ka)	Reduced chi-squared	Boulder	Published ^{10}Be CRE age (ka)	Recalculated ^{10}Be CRE age (ka)	Original reference	Comments
Wormsa valley (Vosges)	Outer moraine	14.4±1.6	-	-	W7	9.0±1.7†	14.4±1.6	Mercier *et al.* (1999)	Coordinates of the sampling sites were determined in www.geoportail.fr (last access: 8 June 2021) with information from a fieldwork report (Braucher R, unpublished data); topographic shielding factors were calculated with the toolbox of Li (2018) and a digital terrain model (DTM) acquired during the shuttle radar topography mission (SRTM; NASA Jet Propulsion Laboratory, 2013); As the sample thickness was ≤3 cm (Braucher R, personal communication, 14 February 2020), a sample thickness of 3 cm was assumed for CRE age calculations.
	Inner moraine	13.6±1.6	-	-	W8	8.3±1.6†	13.6±1.6		
Altenbach valley/Missheimle cirque (Vosges)	Moraine	22.5±1.9	23.7±2.2	-	A6a	14.4±2.5†	21.3±1.6		
					A6b	15.3±2.8†	23.7±2.2		
	Outer moraine in the cirque	19.3±1.5	20.1±1.5	-	M5a	11.5±2.0†	20.1±1.5		
					M5c	11.5±2.0†	18.4±1.5		
	Inner moraine in the cirque	16.8±1.5	17.7±1.5	-	M5b	10.6±1.9†	17.7±1.5		
					M5e	10.6±1.9†	15.9±1.5		
Lac Noir cirque (Vosges)	Moraine	14.7±1.5	-	-	Ln2	9.7±1.8†	14.7±1.5		

Locality	Landform	Landform age (ka)	Oldest ^{10}Be CRE age (ka)	Reduced chi-squared	Boulder	Published ^{10}Be CRE age (ka)	Recalculated ^{10}Be CRE age (ka)	Original reference	Comments
Aare valley (foreland of the Alps)	Moraine at Steinhof	22.9±1.4	23.3±1.5	0.40	ER-1	18.9±1.5	23.3±1.5	Ivy-Ochs *et al.* (2004)	
					ER-2	19.4±1.3	23.5±1.2		
					ER-8	17.9±1.4	22.0±1.4		
	Gurten stade moraine	19.5±1.3	19.9±1.6	5.43	GS1	20.7±2.2	19.9±1.6	Wüthrich *et al.* (2018)	
					GS3	19.8±1.7	19.1±1.0		
					GS5	18.2±1.5	17.5±0.6		
	Bern stade moraine	17.4±0.8	18.4±1.4	7.76	BS2	19.0±2.0	18.4±1.4		
					BS3	16.7±1.5	15.9±0.8		
					BS4	15.6±1.3	14.9±0.6		
					BS5	18.4±1.5	17.6±0.6		
					BS6	18.7±1.5	17.9±0.6		
Lenzburg/Wohlen (foreland of the Alps)	Moraine at Lenzburg	21.5±1.0	-	-	Reuss-21	22.0±0.9	21.5±1.0	Reber *et al.* (2014)	

Locality	Landform	Landform age (ka)	Oldest ^{10}Be CRE age (ka)	Reduced chi-squared	Boulder	Published ^{10}Be CRE age (ka)	Recalculated ^{10}Be CRE age (ka)	Original reference	Comments
	Moraine at Wohlen	18.2±1.0	-	-	Reuss-20	18.6±0.9	18.2±1.0		
Lake Starnberg (foreland of the Alps)	Maximum moraine	17.7±1.0	19.5±1.1	1.96	AVS-03-01	16.9‡	19.5±1.1	Reuther (2007)	Coordinates of the sampling sites and topographic shielding factors from Ivy-Ochs *et al.* (2008).
					AVS-03-06	15.6‡	18.0±1.1		
					AVS-03-11	14.4‡	16.6±1.0		
					AVS-03-22	14.5‡	16.8±1.0		
	Inner moraine	18.1±1.2	19.4±1.0	-	AVS-03-03	16.7‡	19.4±1.0		
					AVS-03-04	14.6‡	16.9±1.4		
Gschnitz valley (Eastern Alps)	Moraine at Trins	17.9±1.0	19.2±0.8	1.75	Gamma 3	14.6±0.8	17.6±1.0	Ivy-Ochs *et al.* (2006a)	Coordinates of the sampling sites from Ivy-Ochs *et al.* (2006b).
					Gamma 5	14.5±1.1	17.6±1.3		
					Gamma 8a	15.5±1.0	19.2±0.8		
					Gamma 103	14.0±0.6	17.2±0.7		

Locality	Landform	Landform age (ka)	Oldest ^{10}Be CRE age (ka)	Reduced chi-squared	Boulder	Published ^{10}Be CRE age (ka)	Recalculated ^{10}Be CRE age (ka)	Original reference	Comments
Kleiner Arbersee (Bavarian Forest)	W1a moraine	21.0±1.0	22.3±0.9	2.10	BW-03-15	19.5‡	22.3±0.9	Reuther (2007)	
					BW-03-14	17.4‡	19.9±1.4		
					BW-03-16	18.0‡	20.7±0.8		
	W1b moraine	20.3±1.0	20.3±1.0	-	BW-03-06	17.6‡	20.3±1.0		
					BW-03-02	17.6‡	20.3±0.9		
	W2 moraine	18.8±0.8	18.8±0.9	-	BW-03-03	16.4‡	18.8±0.9		
					BW-03-20	16.2‡	18.7±0.8		
	Lake moraine	16.9±1.1	17.3±1.7	0.67	BW-04-03	14.9‡	17.2±0.9		
					BW-04-04	15.0‡	17.3±1.7		
					BW-03-09	14.1‡	16.2±0.7		
Laka valley (Bohemian Forest)	Laka1 moraine	15.8±1.8	-	-	LA-2	16.3±1.9	15.8±1.8	Mentlík *et al.* (2013)	
	Laka2 moraine	13.8±1.3	-	-	LA-1	14.1±1.3	13.8±1.3		

Locality	Landform	Landform age (ka)	Oldest ^{10}Be CRE age (ka)	Reduced chi-squared	Boulder	Published ^{10}Be CRE age (ka)	Recalculated ^{10}Be CRE age (ka)	Original reference	Comments
Prášilské valley (Bohemian Forest)	Pras1 moraine	17.5±1.4	19.0±2.2	1.03	PR-6	17.1±1.1	16.6±1.1		
					PR-7	19.5±2.3	19.0±2.2		
					PR-8	17.1±0.8	16.7±0.9		
	Pras2 moraine	15.4±0.7	15.8±0.7	0.43	PR-2	15.7±0.7	15.4±0.8		
					PR-3	16.2±0.6	15.8±0.7		
					PR-1	15.4±0.6	15.0±0.6		
	Pras3 moraine	13.4±1.2	13.9±0.9	-	PR-4	14.2±0.9	13.9±0.9		
					PR-5	13.1±1.5	12.9±1.5		
Snowy cirques (Giant Mountains)	SK-I moraine	18.4±1.0	-	-	SK-16	20.8±1.0	18.4±1.0	Engel *et al.* (2014)	Coordinates of the sampling sites from Krause D (personal communication, 8 June 2021)
	SK-II moraine	18.1±0.9	-	-	SK-03	19.5±0.9	18.1±0.9		
	SK-III moraine	18.4±0.7	18.5±0.7	-	SK-08	21.2±0.7	18.5±0.7		
					SK-09	20.9±0.6	18.3±0.7		

Locality	Landform	Landform age (ka)	Oldest ^{10}Be CRE age (ka)	Reduced chi-squared	Boulder	Published ^{10}Be CRE age (ka)	Recalculated ^{10}Be CRE age (ka)	Original reference	Comments
	SK-IV moraine	13.6±1.2	16.0±0.7	-	SK-05	12.7±2.0	11.2±1.8		
					SK-07	18.1±0.6	16.0±0.7		
	SK-VI moraine	12.0±0.5	-	-	SK-06	13.5±0.5	12.0±0.5		
	SK-VII moraine	11.5±0.7	11.6±0.6	-	SK-01	12.7±0.9	11.3±0.8		
					SK-02	13.1±0.5	11.6±0.6		
Labský důl (Giant Mountains)	Terminal moraine	17.5±1.5	17.8±1.6	-	LN-19	12.1±2.1	17.8±1.6	Mercier *et al.* (2000)	Coordinates of the sampling sites from Krause D (personal communication, 8 June 2021); topographic shielding factors calculated with the toolbox of Li (2018) and a SRTM-DTM (NASA Jet Propulsion Laboratory, 2013)
					LN-20	11.5±2.0	17.1±1.5		
Łomnica valley (Giant Mountains)	Second outermost moraine	16.9±1.0	-	-	Lo-7	16.0±0.9	16.9±1.0	Engel *et al.* (2011)	
	Third outermost moraine	16.8±0.8	-	-	Lo-6	15.9±0.6	16.8±0.8		
	Fourth outermost moraine	17.4±0.8	-	-	Lo-5	16.5±0.6	17.4±0.8		

Locality	Landform	Landform age (ka)	Oldest ^{10}Be CRE age (ka)	Reduced chi-squared	Boulder	Published ^{10}Be CRE age (ka)	Recalculated ^{10}Be CRE age (ka)	Original reference	Comments
	Third innermost moraine	17.5±0.6	-	-	Lo-3	17.0±0.4	17.5±0.6		
	Innermost moraine	15.4±0.6	-	-	Lo-4	14.8±0.5	15.4±0.6		
	Second innermost moraine (southern part of the cirque)	13.7±0.9	-	-	Lo-2	13.6±0.9	13.7±0.9		
Úpa valley (Giant Mountains)	G-I moraine	14.7±0.8	17.2±0.7	4.91	G-18	16.4±0.5	15.1±0.6	Engel *et al.* (2014)	Coordinates of the sampling sites from Krause D (personal communication, 8 June 2021)
					G-19	18.9±0.6	17.2±0.7		
					G-20	14.8±1.1	13.6±1.1		
					G-21	16.7±0.6	15.3±0.6		
	G-II moraine	14.3±1.2	16.1±1.8	1.83	G-10	14.8±1.0	13.6±0.9		
					G-11	17.6±2.0	16.1±1.8		
					G-12	14.3±0.9	13.1±0.9		

Locality	Landform	Landform age (ka)	Oldest ^{10}Be CRE age (ka)	Reduced chi-squared	Boulder	Published ^{10}Be CRE age (ka)	Recalculated ^{10}Be CRE age (ka)	Original reference	Comments
	G-III moraine	15.9±0.6	17.6±0.7	-	G-17	19.0±0.7	17.6±0.7		
					G-24	16.6±0.6	14.2±0.6		
	G-IV moraine	15.1±0.6	16.7±0.7	-	G-15	14.6±0.5	13.5±0.6		
					G-16	18.2±0.7	16.7±0.7		
	G-V moraine	14.0±0.6	14.5±0.6	-	G-13	15.0±0.5	13.6±0.5		
					G-14	15.7±0.5	14.5±0.6		
Łomniczka valley (Giant Mountains)	Moraine	15.1±0.7	-	-	Lk-1	14.3±0.6	15.1±0.7	Engel *et al.* (2011)	

[†]Mercier *et al.* (1999) only reported CRE ages corrected for seasonal snow cover.

[‡] Reuther (2007) did not report the uncertainty of the CRE ages which were not corrected for erosion or snow shielding.

References

Balco G. 2007. CRONUS-Earth Al-26/Be-10 exposure age calculator MATLAB function reference Version 2: November, 2007. http://hess.ess.washington.edu/math/docs/al_be_v2/al_be_fctn_desc/ [15 July 2021].

Balco G. 2018. Topographic shielding calculator. http://stoneage.ice-d.org/math/skyline/skyline_in.html [27 August 2020].

Balco G, Stone JO, Lifton NA, et al. 2008. A complete and easily accessible means of calculating surface exposure ages or erosion rates from ^{10}Be and ^{26}Al measurements. *Quaternary Geochronology* **3** (3): 174–195 [DOI: 10.1016/j.quageo.2007.12.001].

Claude A, Ivy-Ochs S, Kober F, et al. 2014. The Chironico landslide (Valle Leventina, southern Swiss Alps): age and evolution. *Swiss Journal of Geosciences* **107** (2): 273–291 [DOI: 10.1007/s00015-014-0170-z].

Engel Z, Braucher R, Traczyk A, et al. 2014. ^{10}Be exposure age chronology of the last glaciation in the Krkonoše Mountains, Central Europe. *Geomorphology* **206**: 107–121 [DOI: 10.1016/j.geomorph.2013.10.003].

Engel Z, Traczyk A, Braucher R, et al. 2011. Use of ^{10}Be exposure ages and Schmidt hammer data for correlation of moraines in the Krkonoše Mountains, Poland/Czech Republic. *Zeitschrift für Geomorphologie* **55** (2): 175–196 [DOI: 10.1127/0372-8854/2011/0055-0036].

Ivy-Ochs S, Kerschner H, Kubik PW, et al. 2006a. Glacier response in the European Alps to Heinrich Event 1 cooling: the Gschnitz stadial. *Journal of Quaternary Science* **21** (2): 115–130 [DOI: 10.1002/jqs.955].

Ivy-Ochs S, Kerschner H, Reuther A, et al. 2006b. The timing of glacier advances in the northern European Alps based on surface exposure dating with cosmogenic ^{10}Be, ^{26}Al, ^{36}Cl, and ^{21}Ne. In *In Situ-Produced Cosmogenic Nuclides and Quantification of Geological Processes*, Siame LL, Bourlès DL, Brown ET (eds). Geological Society of America: Boulder; 43–60.

Ivy-Ochs S, Kerschner H, Reuther A, et al. 2008. Chronology of the last glacial cycle in the European Alps. *Journal of Quaternary Science* **23** (6-7): 559–573 [DOI: 10.1002/jqs.1202].

Ivy-Ochs S, Schäfer J, Kubik PW, et al. 2004. Timing of deglaciation on the northern Alpine foreland (Switzerland). *Eclogae Geologicae Helvetiae* **97** (1): 47–55 [DOI: 10.1007/s00015-004-1110-0].

Lal D. 1991. Cosmic ray labeling of erosion surfaces: in situ nuclide production rates and erosion models. *Earth and Planetary Science Letters* **104** (2-4): 424–439 [DOI: 10.1016/0012-821X(91)90220-C].

Li Y-K. 2018. Determining topographic shielding from digital elevation models for cosmogenic nuclide analysis: a GIS model for discrete sample sites. *Journal of Mountain Science* **15** (5): 939–947 [DOI: 10.1007/s11629-018-4895-4].

Martin LCP, Blard PH, Balco G, et al. 2017. The CREp program and the ICE-D production rate calibration database: A fully parameterizable and updated online tool to compute cosmic-ray exposure ages. *Quaternary Geochronology* **38**: 25–49 [DOI: 10.1016/j.quageo.2016.11.006].

Mentlík P, Engel Z, Braucher R, et al. 2013. Chronology of the Late Weichselian glaciation in the Bohemian Forest in Central Europe. *Quaternary Science Reviews* **65**: 120–128 [DOI: 10.1016/j.quascirev.2013.01.020].

Mercier J-L, Bourlès DL, Kalvoda J, et al. 1999. Deglaciation of the Vosges dated using ^{10}Be. *Acta Universitatis Carolinae Geographica* **2**: 139–155.

Mercier J-L, Kalvoda J, Bourlès DL, et al. 2000. Preliminary results of ^{10}Be dating of glacial landscape in the Giant Mountains. *Acta Universitatis Carolinae Geographica, Supplementum* **35**: 157–170.

Muscheler R, Beer J, Kubik PW, et al. 2005. Geomagnetic field intensity during the last 60,000 years based on ^{10}Be and ^{36}Cl from the Summit ice cores and ^{14}C. *Quaternary Science Reviews* **24** (16): 1849–1860 [DOI: 10.1016/j.quascirev.2005.01.012].

NASA Jet Propulsion Laboratory. 2013. NASA Shuttle Radar Topography Mission Global 1 arc second. https://doi.org/10.5067/MEaSUREs/SRTM/SRTMGL1.003 [31 May 2021].

Nishiizumi K, Winterer EL, Kohl CP, et al. 1989. Cosmic ray production rates of ^{10}Be and ^{26}Al in quartz from glacially polished rocks. *Journal of Geophysical Research: Solid Earth* **94** (B12): 17907–17915 [DOI: 10.1029/JB094iB12p17907].

Reber R, Akçar N, Ivy-Ochs S, et al. 2014. Timing of retreat of the Reuss Glacier (Switzerland) at the end of the Last Glacial Maximum. *Swiss Journal of Geosciences* **107** (2): 293–307 [DOI: 10.1007/s00015-014-0169-5].

Reuther AU. 2007. *Surface exposure dating of glacial deposits from the last glacial cycle. Evidence from the Eastern Alps, the Bavarian Forest, the Southern Carpathians and the Altai Mountains.* Borntraeger: Berlin, Stuttgart.

Spencer CJ, Yakymchuk C, Ghaznavi M. 2017. Visualising data distributions with kernel density estimation and reduced chi-squared statistic. *Geoscience Frontiers* **8** (6): 1247–1252 [DOI: 10.1016/j.gsf.2017.05.002].

Stone JO. 2000. Air pressure and cosmogenic isotope production. *Journal of Geophysical Research: Solid Earth* **105** (B10): 23753–23759 [DOI: 10.1029/2000JB900181].

Uppala SM, Kållberg PW, Simmons AJ, et al. 2005. The ERA-40 re-analysis. *Quarterly Journal of the Royal Meteorological Society* **131** (612): 2961–3012 [DOI: 10.1256/qj.04.176].

Wüthrich L, Morabito EG, Zech J, et al. 2018. ^{10}Be surface exposure dating of the last deglaciation in the Aare Valley, Switzerland. *Swiss Journal of Geosciences* **111** (1): 295–303 [DOI: 10.1007/s00015-018-0298-3].